*Macromolecules* **1996,** *29,* 7683−7689

# Polymerization-Induced Phase Separation. 1. Conversion−Phase Diagrams

**H. M. J. Boots,* J. G. Kloosterboer, C. Serbutoviez, and F. J. Touwslager**

*Philips Research Laboratories, Professor Holstlaan 4, 5656 AA Eindhoven, The Netherlands*

*Received February 22, 1996; Revised Manuscript Received August 12, 1996*[⊗]

ABSTRACT: A thermodynamic model is given for phase separation induced by the increase of network elasticity during free-radical cross-linking polymerization. The importance of network elasticity in the field of polymer dispersed liquid crystals is stressed. The concept of a conversion−phase diagram is introduced as an attractive way to visualize the onset of phase separation in all situations where the phase separation is induced by polymerization. The results of the model are presented in conversion−phase diagrams.

## 1. Introduction

Over the past decade, cells containing nematic liquid crystal (LC) in a polymer matrix have become a viable alternative for twisted nematic cells in a number of applications. The most studied systems of this kind are polymer dispersed liquid crystals (PDLCs).[1−3] In PDLCs, the polymer matrix is optically isotropic with a refractive index matching the ordinary refractive index of the liquid crystal in the dispersed phase. If no voltage is applied, the cell scatters light; if a sufficiently high voltage is applied across the cell, the director in the LC droplets turns parallel to the field and the cell is transparent for perpendicularly incident light.

One of the techniques to produce PDLCs is polymerization-induced phase separation (PIPS). In this technique, polymerization is started in a mixture of monomer and LC. Due to the polymerization, the system separates into two phases. Most of the polymer belongs to one of these phases: the matrix phase. Most of the LC and the unreacted monomer is present in the other phase, which will be denoted as the LC phase. Conditions are often chosen such that the LC phase appears as separate droplets in the matrix phase. The coalescence of these droplets is impeded by the cross-links in the matrix or, in the case of linear polymerization, by vitrification of the matrix. In the later stages of the polymerization, the size and shape of the LC regions will hardly change anymore.

In the models of PIPS for PDLCs it is often assumed that the phase separation occurs as a result of the increasing size of the growing polymer molecules.[4−6] This may be correct for linear polymerization, in which case no network is present, and also in the first part of cross-linking polymerization by step reactions. However, in the often applied cross-linking polymerization by chain reactions, gelation may occur well before phase separation sets in, as will be shown to be the case in the experiments of paper 2 of this series.[7] In such a situation one has an infinite network almost from the start of the reaction and phase separation can be induced by the increasing elasticity of the swollen network during polymerization.

In this paper we emphasize the importance of elasticity in the thermodynamics of polymerization-induced phase separation. Thermodynamics does not yield information on the size and morphology of the regions of different phases, but it does predict the compositions of the two phases and some aspects of the structure of the polymer network.

Although network elasticity has not been modeled in the literature on PIPS in connection to PDLCs, a rich old literature exists on swelling equilibria in polymer networks and even on elasticity-induced phase separation during polymerization. Some of the outstanding early contributions to this field are given in refs 8−14. The elastic contribution to the Gibbs free energy of the system is the subject of rubber elasticity theory; a field of lively discussions over the last few decades.[15,16] New impulses have come from computer simulations of the elastic behavior of networks of chosen topology.[16] The model that we will present here is in its simplest form identical to the 1967 model by Dušek.[13] The extensions to incorporate developments of rubber elasticity after 1967 will be shown not to change the qualitative features of the model.

The intention of this paper is to present these existing ideas in an accessible way to researchers in the field of PDLCs and of polymers as a basis for the interpretation of the experiments in part 2 of this series.[7] To this purpose, we will use the concept of a conversion−phase diagram as a means to visualize the results on phase separation during polymerization. It combines the thermodynamics of the three-component system (monomer, polymer, and solvent) with the conversion of monomer molecules into polymer repeat units. Furthermore, we will go into detail in explaining the sweeping assumptions that have to be made to apply the model to PDLC formation by PIPS. The general framework presented here may also serve in the interpretation of phase separation phenomena during the processing of linear polymers in reactive solvents.[17]

This paper only discusses the simplest phase behavior: in the beginning there is one phase, containing a network. At phase separation, the polymer network deswells and a new phase appears that contains only LC and monomer. In more complicated situations, two phases, both containing polymer, could develop by phase separation induced by the Flory−Huggins interaction parameter $\chi$, before a phase without polymer appears (in ref 18 such a situation is discussed for the case of temperature decrease instead of ongoing polymerization). The description of these situations remains a challenge, since in two coexisting network phases the rate of polymerization as well as the rate of cross-linking is different.

In section 2 the thermodynamics of PIPS is presented. In section 3 and 4 the applicability to step and chain

---

[⊗] Abstract published in *Advance ACS Abstracts,* October 15, 1996.

S0024-9297(96)00292-6 CCC: $12.00

reaction processes is discussed. The concept of conversion−phase diagrams is introduced in section 5 and typical examples of such diagrams and of regular three-component phase diagrams are presented for our model in section 6. Section 7 summarizes the results.

## 2. Thermodynamics

In describing phase separation in polymerizing systems, we assume that thermodynamic equilibrium is attained after each reaction step, so that a thermodynamic treatment is valid. This assumption is motivated by the fact that each reaction step constitutes only a local disturbance of thermodynamic equilibrium. The Gibbs free energy is a function of the volume fractions $\phi_M$, $\phi_S$, and $\phi_P$ of the three components: monomer (M), solvent (S), and polymer network (P).

Nowhere will we use the LC character of the solvent, although for the PDLC application the droplets must be nematic in the temperature range of operation. In some systems of interest, the isotropic−nematic transition is found to occur by monomer depletion in the LC rich phase *after* the primary phase separation into a network phase and an LC rich phase. In other systems it may occur simultaneously, but the nematic term in the free energy does not induce the phase separation. Therefore, it is not essential in a qualitative description. In a more complete description, elasticity would be added to models for LC solutions.[19]

Polymerization-induced phase separation may occur for three reasons.[12,13] The first reason is the increasing fraction of large molecules during polymerization (size-induced phase separation). It is well-known that size-induced phase separation can only occur if $\chi/k_BT$ is in the appropriate range. A second reason is that the $\chi$ parameter between monomer and solvent may be different from the $\chi$ parameter between polymer and solvent; in this case, the increasing fraction of polymer may cause phase separation by the combined effect of size-induced and $\chi$-induced phase separation. In the case of cross-linking polymerization, the elasticity of the network is a third driving force for phase separation. It may induce phase separation—even if all interaction parameters are zero—due to the increase of the gel fraction and the number of cross-links. In this case one speaks of deswelling of the polymer network: a new phase without polymer network is formed.

Our model, which dates back to Dušek,[13] is based on the following assumptions:

(i) Mixing and elasticity contribute independently to the Gibbs free energy:

$$\Delta G = \Delta G^{\mathrm{mix}} + \Delta G^{\mathrm{el}} \qquad (1)$$

(As usual in thermodynamics, $\Delta G$ refers to the difference between the actual Gibbs free energy and the standard Gibbs free energy, which is the average of the Gibbs free energies of the pure components.) This assumption dates back to Flory and Rehner.[9] It has been criticized in refs 20 and 21.

(ii) The mixing of solvent, monomer, and polymer is described by the model of Flory, Huggins, Staverman, and Van Santen[22] with concentration independent interaction parameters $\chi_{ij}$. For our three-component system, the Flory−Huggins term is given by[22,24]

$$\frac{\Delta G^{\mathrm{mix}}}{Nk_BT} = \phi_M \log \phi_M + \phi_S \log \phi_S + \frac{\phi_P}{r_P} \log \phi_P + \sum_{ij} \chi_{ij}\phi_i\phi_j \qquad (2)$$

where the summation runs over $(i, j) = (\mathrm{M, S}), (\mathrm{M, P})$, and $(\mathrm{S, P})$. $r_P$ is the degree of polymerization, $k_B$ is Boltzmann's constant, and $T$ is the absolute temperature; $\chi_{ij}$ is the coefficient of the interaction between particles of type $i$ and $j$. It has often been shown that the Flory−Huggins model only provides a good fit with experiment if $\chi_{ij}$ may depend on the temperature and the concentrations and sizes of the components. We do not take these dependencies into account in order not to increase the complexity of the equations and the number of parameters. For simplicity of notation, we also assume that monomer molecules, solvent molecules, and monomer repeat units in the polymer all have the same size. In that case $N$ is the total number of these molecules and repeat units in the system. The equation for molecules of different sizes is given in the Appendix.

The Flory−Huggins contribution to the monomer chemical potential is obtained by differentiation of $\Delta G^{\mathrm{mix}}$ with respect to the number $N_M$ of monomer molecules[22,24] at constant pressure, temperature, and numbers of polymer and solvent molecules:

$$\begin{aligned}\Delta\mu_M^{\mathrm{mix}}/(k_BT) &= \frac{\partial}{\partial N_M}\Delta G^{\mathrm{mix}}/(k_BT)\\ &= \log \phi_M + \left(1 - \frac{1}{r_P}\right)\phi_P + [\chi_M(1-\phi_M)^2 + \\ &\qquad \chi_P{\phi_P}^2 + \chi_S{\phi_S}^2] \qquad (3)\end{aligned}$$

and similarly for $\Delta\mu_S^{\mathrm{mix}}$, the Flory−Huggins contribution to the solvent chemical potential. The $\chi$ parameters are given by

$$\chi_M = \frac{1}{2}(\chi_{MP} + \chi_{MS} - \chi_{PS}) \qquad (4)$$

and similarly for $\chi_P$ and $\chi_S$.

(iii) The standard expression for the elastic contribution to the Gibbs free energy per molecule is[12,13,18]

$$\frac{\Delta G^{\mathrm{el}}}{Nk_BT} = \frac{\nu_e}{N}\left[\frac{3}{2}A{\Phi_P}^{2/3}({\phi_P}^{-2/3} - 1) + B \ln \phi_P\right] \qquad (5)$$

Here $\nu_e$ is the number of elastically active network chains. For ideal networks $\nu_e$ is related to the network chain length $m_c$ (measured in repeat units) between cross-links by[18] $\nu_e/N = \phi_P/m_c$. If there is a distribution of the number of repeat units between cross-links, ${m_c}^{-1}$ is replaced by the weight average of ${m_c}^{-1}$. $\Phi_P$ is defined as the polymer fraction $\phi_P$ at the moment of cross-linking. The factor $(\Phi_P/\phi_P)^{-2/3}$ is a rewriting of the ratio $\langle R^2\rangle_{\mathrm{act}}/\langle R^2\rangle_{\mathrm{xl}}$ of the actual size of a network chain after swelling or deswelling and of the size of the network at the moment that it has been made. These notions are well-known from the cross-linking of primary chains. If the primary chains are cross-linked in the bulk, $\Phi_P = 1$. For cross-linking polymerization we also use eq 5, although not all chains between cross-links are so long to be Gaussian. Part of the error introduced by this assumption may be corrected for by an effective value of $m_c$. We assume that at the formation of each new cross-link, the network remains homogeneous, so that one does not have "old" and "new" portions of a network. Therefore $\Phi_P$ remains equal to $\phi_P$ during polymerization, up to the point of phase separation.

From eq 5 we find the following elastic contribution to the chemical potentials

$$\Delta\mu_{\mathrm{M}}^{\mathrm{el}}/(k_{\mathrm{B}}T) = \Delta\mu_{\mathrm{S}}^{\mathrm{el}}/(k_{\mathrm{B}}T) = m_{\mathrm{c}}^{-1}[A(\Phi_{\mathrm{P}}/\phi_{\mathrm{P}})^{2/3} - B]\phi_{\mathrm{P}} \tag{6}$$

Differences between elasticity models amount to different expressions for $A$ and $B$ in eqs 5 and 6. Here we use the affine model[13,22]

$$A = 1 \qquad B = 2/f \tag{7}$$

where $f$ is the functionality of the cross-links.[23] In the other classic model of rubber elasticity, the phantom-network model,[8] one has $B = 0$. In more recent models of network elasticity,[15] $A$ and $B$ depend on the polymer volume fraction. In the Appendix we discuss the qualitative effect of such models.

All of the assumptions in this section have been subject to dispute in the literature.

## 3. Cross-Linking Polymerization by Step Reactions

During polymerization by step reactions, the average size of the molecules increases continuously until the gel point. Therefore, size-induced phase separation is likely to occur before the gel point is reached. If, however, phase separation occurs after the gel point, the elasticity of the network should be taken into account. One may expect a broad distribution of molecular sizes at phase separation, unless it occurs near the very end of the reaction. This complicates the modeling of elasticity-induced phase separation during step reaction polymerization. The simpler problem of mixing a solvent with a network formed by a step reaction has been modeled by Dušek.[26]

## 4. Free-Radical Polymerization of Divinyl Monomer

The application of the model of section 2 to polymerization of tetrafunctional monomer by a chain reaction has consequences for both the mixing and the elastic terms in the chemical potentials. In the mixing terms, one may take the polymer size $r_{\mathrm{P}}$ infinite, since in the usual experimental situation the radical concentration is so low that there is always only a negligible concentration of polymer particles containing less than, e.g., 10 units.[27]

The elastic contribution to the chemical potentials is more accurate for vulcanization of linear chains than for cross-linking polymerization. It is based on the assumption of a ring-free network of Gaussian chains. In chain-reaction cross-linking polymerization, densely cross-linked microgel particles are formed, containing many rings that do not contribute to the elasticity. Moreover, the chain length between cross-links will not always be so large as to justify a Gaussian distribution of the end-to-end distance. Dušek[28] has estimated that the cross-linking efficiency may be as low as 1% in vinyl/divinyl systems containing relatively high fractions of divinyl. Nevertheless, we will apply eq 7 to the case of chain reactions. The reasons are that many PIPS experiments for PDLC, including the ones of paper 2, use chain reactions and that a better model of the elasticity of networks obtained by chain reactions can only be formulated after a large experimental and a huge computational effort. But here we want to stress the qualitative nature of the results that will be obtained.

In the model experiments of paper 2, the monomer is a pure divinyl compound that is converted into a cross-linked polymer through UV-induced free-radical polymerization. Hence the functionality $f = 4$. In these experiments it is not possible to determine the average of $m_{\mathrm{c}}^{-1}$ independently. Therefore we use the following crude mean-field estimate:[13]

$$m_{\mathrm{c}}^{-1} = x^2/\alpha = [2 - \alpha - 2\sqrt{1-\alpha}]/\alpha \tag{8}$$

where $\alpha$ is the conversion of monomer (the fraction of monomer molecules converted into polymer repeat units), $x$ is the conversion of reactive groups, and $x^2$ is the probability for a unit to be a cross-link, so that $x^2/\alpha$ is the fraction of cross-links among reacted units.

Mean-field models of free-radical cross-linking polymerization have been criticized, since they do not account for spatial inhomogeneity.[30−35] Experimental evidence has been found of microgel particles. They may be created by microphase separation, but the mere physical kinetics of the chain reaction process leads also to microgel particles.[34] These particles are highly internally cross-linked and loosely connected. It is not known how the elasticity of such networks should be described. We compare two *ad hoc* ways to account for the specific character of chain reactions.

(A) We add an overall efficiency factor $\epsilon < 1$ to the elastic terms in the chemical potential to account for the large fraction of elastically ineffective network chains. So for model A eq 7 reads

$$\Delta\mu_{\mathrm{M}}^{\mathrm{el}}/(k_{\mathrm{B}}T) = \Delta\mu_{\mathrm{S}}^{\mathrm{el}}/(k_{\mathrm{B}}T) = \epsilon(x^2/\alpha)[(\Phi_{\mathrm{P}}/\phi_{\mathrm{P}})^{2/3} - 1/2]\phi_{\mathrm{P}} \tag{9}$$

(B) We consider the loosely connected microgel particles as effective cross-links of functionality $f = \infty$. The limit of infinite functionality for most models of network elasticity leads to the phantom network model that was proposed by James and Guth for any functionality.[8] The wastage of real cross-links in the microgel particles is again described by the efficiency factor $\epsilon$. The number of microgel particles is hard to model. In the beginning of the reaction, one could assume that one has as many microgel particles as initiated chain reactions, but in a later stage one could get coalescence of microgel particles. Models of this kind would be highly speculative. Lacking any better model thus far, and lacking any experimental data on the number of elastically active network chains for the system of our interest, we continue to use eq 8 for $m_{\mathrm{c}}$, as it qualitatively describes the increase of the number of effective cross-links during reaction. Any deviation is assumed to be described by the efficiency factor. So for model B:

$$\Delta\mu_{\mathrm{M}}^{\mathrm{el}}/(k_{\mathrm{B}}T) = \Delta\mu_{\mathrm{S}}^{\mathrm{el}}/(k_{\mathrm{B}}T) = \epsilon(x^2/\alpha)\Phi_{\mathrm{P}}^{2/3}\phi_{\mathrm{P}}^{1/3} \tag{10}$$

During polymerization $\phi_{\mathrm{P}} = \Phi_{\mathrm{P}}$, so that in the conversion−phase diagram, model A with efficiency factor $\epsilon$ is equivalent to model B with efficiency factor $\epsilon/2$.

The combination of the assumptions in both this section and section 2 leads to a model that is not suited for quantitative predictions. However, the model does help in qualitative interpretations of experimental data on phase separation during network formation by chain reactions. This will be apparent in paper 2 of this series.

If cross-linking polymerization is started in a monomer−solvent solution, phase separation may occur either before or after gelation. Only if it occurs after gelation may elasticity play a role. The common situation for free-radical cross-linking polymerization is that the initiation rate is low. In that case the gel point of bulk polymerization of divinyl monomer is far below 1% conversion, even though the formation of microgel particles tends to raise the gel point conversion. One may increase the gel point conversion by increasing the concentration of the monovinyl compound in the copolymerization of mono- and divinyl monomer, by diluting the polymerizing system, by adding transfer agents, or by increasing the initiation rate.[30,36] In this way one can create conditions under which the elasticity does or does not contribute to the phase separation. In paper 2, we show that under common experimental conditions gelation precedes the phase transition and elasticity is important.

In our model gelation occurs at infinitely small conversion: we have initially one phase, and this phase contains a system-spanning network. Since in the model an infinitely dilute network is present at infinitely small conversion, there is a discontinuity on the MS axis. This discontinuity models the fast buildup of elasticity in the first moments of polymerization.

## 5. Conversion−Phase Diagrams

The following relations hold between the conversion $\alpha$ and the overall volume fractions:

$$\phi_M = (1 - \alpha)(1 - \phi_S) \tag{11}$$

$$\phi_P = \alpha(1 - \phi_S) \tag{12}$$

Thus the polymerization may be described in a triangular M−P−S diagram as a line of constant solvent concentration (line AB in Figure 1a). We shall call such a diagram a conversion−phase diagram. A line of constant solvent concentration (parallel to the M−P side) will be called a polymerization line; along such a line the conversion increases from left to right.

In Figure 1a the polymerization line AB at $\phi_S = 0.6$ is drawn. Just after the start of the reaction, the system has gelled and we have one phase containing the network, the monomer, and the solvent. On further polymerization, the network becomes more and more cross-linked. At some point (point X in the diagram) it will deswell: a new phase containing only monomer and solvent emerges. The conversion at which this phase separation occurs depends on $\phi_S$. The locus of phase separation points for polymerizations at different solvent fractions is the phase separation curve CD shown in the diagram. Points to the left of this curve refer to single phase systems; points to the right refer to two-phase systems. Thus a conversion−phase diagram is a way to visualize how the onset of phase separation depends on the initial composition of the reaction mixture. A similar type of diagram, called the metastable phase diagram, has been proposed by Mishra *et al.* in the context of simultaneous interpenetrating polymer networks.[29]

It is important to realize what is the difference between a conversion−phase diagram and a phase diagram. In a *phase diagram* the size and structure of the molecules of each component are invariable; each point represents a certain ratio of the components. However, during polymerization the polymer component does not only change in amount, but also in molecular size distribution and/or molecular structure. Therefore, at each point in the *conversion−phase diagram* one has not only a different composition of the system but also a different polymer component. The polymer size and structure at a given point in the conversion−phase diagram depend both on the solvent concentration during polymerization (on which horizontal line the given point is located) and on the conversion (the position of the point on this line).

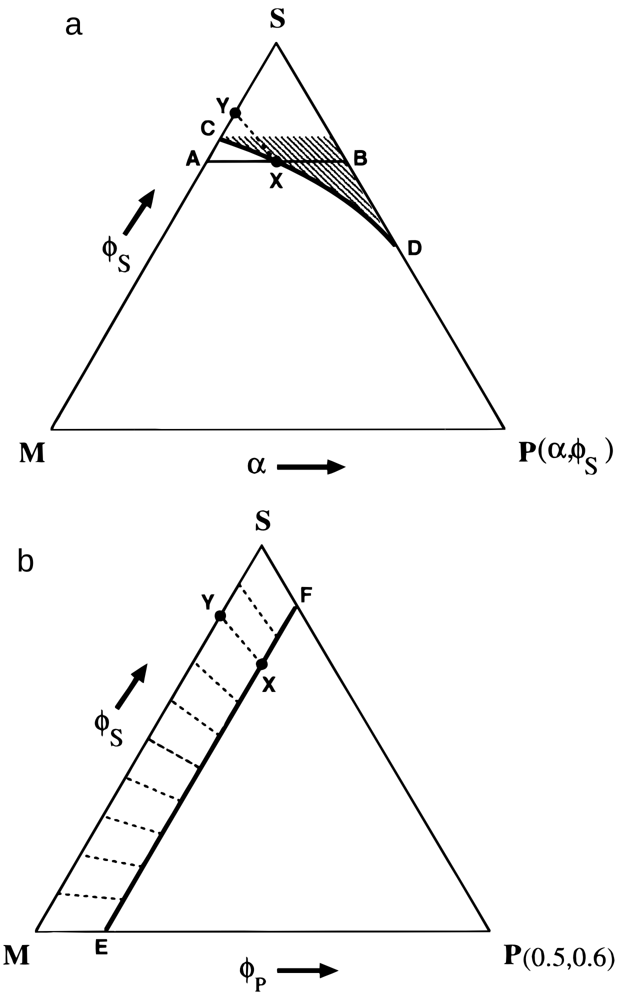

**Figure 1.** (a) Conversion−phase diagram of the polymerization of tetrafunctional monomer M to polymer P in the presence of solvent S for the case $\chi_{MP} = \chi_{MS} = \chi_{PS} = 0$. The arguments of P indicate that the polymer structure depends on the conversion $\alpha$ and on the volume fraction $\phi_S$ of solvent. The curve CD is the phase separation curve. Polymerization occurs from left to right on horizontal lines of constant $\phi_S$ in the diagram. The polymerization line AB at $\phi_S = 0.6$ is drawn; it intersects the phase separation curve at $\alpha = 0.5$ (point *X*). *Y* indicates the composition of the new phase appearing at point *X*. To the right of the phase separation curve (shaded area) two phases are present. (b) Ternary phase diagram of a system polymerized at $\phi_S = 0.6$ until the point of phase separation at $\alpha = 0.5$; $\chi_{MP} = \chi_{MS} = \chi_{PS} = 0$. The polymer structure is determined by the values of $\alpha$ and $\phi_S$ during polymerization and does not change on changing the volume fractions *after polymerization*. Points *X* and *Y* are as in Figure 1a. The thick line EF is the swelling curve. Dashed lines are tie lines.

For each such point in the conversion−phase diagram, *i.e.*, for each polymer structure, one can find a different phase diagram by first stopping the reaction and then changing the solvent or monomer concentrations at *constant* polymer size and structure. As an example, Figure 1b shows the phase diagram of a system that has been polymerized at $\phi_S = 0.6$, until it phase-separated at $\alpha = 0.5$. The polymer structure in that case is determined by the polymerization conditions, but it is independent of the addition or removal of monomer or solvent after the reaction has been stopped.

In the absence of an infinite network, the polymer size (distribution) appears explicitly as $r_P$ in the Flory–Huggins expression eq 3 and implicitly in the $r_P$ dependence of the $\chi$ parameters. In the presence of an infinite network, the polymer structure appears in the elastic chemical potential through $m_c$, which is the number of units between cross-links, and through $\Phi_P$, which is the polymer volume fraction during polymerization. In the mean-field model of eq 8, $m_c$ depends only on the conversion $\alpha$; $\Phi_P$ depends both on the conversion and on the solvent fraction during polymerization.

Imagine the following situation: we start polymerization at $\phi_S = 0$ and halfway through the reaction ($\alpha = 0.5$) we stop the reaction and supply solvent up to a solvent fraction of 0.1. Thus the factor $\Phi_P{}^{2/3}$ in the elastic contribution to the chemical potential is $(0.5)^{2/3}$. This factor is inversely proportional to the mean-square end-to-end distance of the chains between cross-links in the unswollen state. If the polymerization is performed at $\phi_S = 0.1$, this factor is $(0.45)^{2/3}$, so that the elastic contribution is lower. The difference arises from the fact that polymerization is performed in equilibrium: The network polymerized at $\phi_S = 0$ is in a swollen state after dilution to $\phi_S = 0.1$, whereas the network formed at $\phi_S = 0.1$ is not swollen.

## 6. Diagrams for Free-Radical Cross-Linking Polymerization

Phase separation curves in the conversion–phase diagram have been calculated numerically by solving the set of two nonlinear equations for the solvent and monomer chemical potentials in both phases at a fixed value of the monomer conversion $\alpha$:

$$\Delta\mu_M^{\text{phase I}} = \Delta\mu_M^{\text{phase II}} \qquad \Delta\mu_S^{\text{phase I}} = \Delta\mu_S^{\text{phase II}} \tag{13}$$

At a given value of the conversion, the variables in these equations are the volume fractions $\phi_M^{I}$, $\phi_S^{I}$, $\phi_P^{I}$, $\phi_M^{II}$, $\phi_S^{II}$, and $\phi_P^{II}$, of the three components in each phase. The six unknowns can only be determined if four more relations between them are available. Two of these relations are trivial:

$$\phi_M^i + \phi_P^i + \phi_S^i = 1 \qquad (i = \text{I, II}) \tag{14}$$

The third one describes the fact that there is no network in the new phase (phase II).

$$\phi_P^{II} = 0 \tag{15}$$

(We suppose that a network-free phase is separated out first and that polymer created later in that phase is rapidly attached to the network and included in the network phase.) The last equation is

$$\phi_P^{I} = \alpha(1 - \phi_S^{I}) \tag{16}$$

which follows immediately from eq 12 by accounting for the fact that at the moment of phase separation, the volume of phase II is infinitesimal, so that the volume fractions of phase I are equal to the overall volume fractions.

If one wants to calculate the ternary phase diagrams for a specific network structure, one solves the same equations at a given value of the overall polymer volume fraction. In that case, one must also give the polymer structure, *i.e.*, the conversion and the overall solvent fraction at polymerization.

Let us first look at the conversion–phase diagram of model A (with elastic efficiency factor $\epsilon = 1$) for the case that all interaction parameters $\chi$ are equal to zero. Therefore, $\chi$-induced phase separation is impossible and the only reason for phase separation is network elasticity. Another particularity of the zero $\chi$ case is that the network is not preferentially swollen with either monomer or solvent. Therefore, the ratio of monomer and solvent concentrations in either phase is the same. This shows up in the conversion phase diagram in Figure 1a by the fact that the dotted curve that connects the compositions of both phases at phase separation extrapolates to the vertex P in the diagram.

In Figure 1b we plot the ternary phase diagram for swelling and deswelling of a system with zero-valued $\chi$ parameters that has been polymerized at $\phi_S = 0.6$ until it separated into two phases at $\alpha = 0.5$. Here phase separation occurs along a line parallel to the MS edge of the triangle, the swelling line, since in the zero $\chi$ case replacement of a monomer molecule by a solvent molecule does not change the free energy.

The zero $\chi$ case is not very realistic. Although $\chi$ values for the present system have not been measured, experiments on other systems[37,38] suggest that $\chi_{MP}$ may well be of the order of 0.5.

In Figure 2a we plot the conversion–phase diagram of model A for the case that $\chi_{MP} = \chi_{MS} = \chi_{PS} = 0.5$. For linear polymerization (in the absence of elasticity terms) we do not find phase separation ($\chi = 0.5$ is the critical value for chains of infinite length), but we do in the presence of a network. At low solvent concentrations, the equations allow for two values of the conversion at phase separation. We only retain the solution at the lowest conversion, since as soon as phase separation has taken place, the equations do not hold anymore. In Figure 2b we plot the corresponding ternary phase diagram that depicts the phase behavior upon swelling or deswelling of a system that has been polymerized at a solvent fraction of 0.36 until it phase-separated at $\alpha = 0.5$.

For $\chi_{MP} = \chi_{MS} = \chi_{PS} = 0.5$, the introduction of an efficiency factor $\epsilon = 0.1$ in model A (equivalent to model B with $\epsilon = 0.05$) leads to two unconnected physical branches of the phase separation curve, as given in Figure 3. At very low solvent concentrations ($\phi_S < 0.05$) solvent), there is phase separation at very low conversion ($\phi_P < 0.05$). This region does not play a role in PDLC experiments, where high LC concentrations are used to obtain a high volume fraction of the active phase. In the region $0.05\ \phi_S < 0.65$, there is no elasticity-induced phase separation. Then, at fairly high $\phi_S$ ($0.65 < \phi_S < 0.81$), one may again have elasticity-induced phase separation. The phase separation curve is similar to the one in Figure 1a and will be shown to explain qualitative features of phase separation found in the experiments that will be reported in paper 2. At high solvent fractions ($\phi_S > 0.81$), phase separation occurs at infinitesimal conversion according to our model. However, our model does not apply if phase separation precedes gelation. Note, that Figure 3 is qualitative, so that the values of the $\phi_S$ region where elasticity-induced phase separation occurs are not precise.

The large difference between Figures 2a and 3 shows that the contribution of the elastic term is important: a reduction in the efficiency of cross-linking by a factor

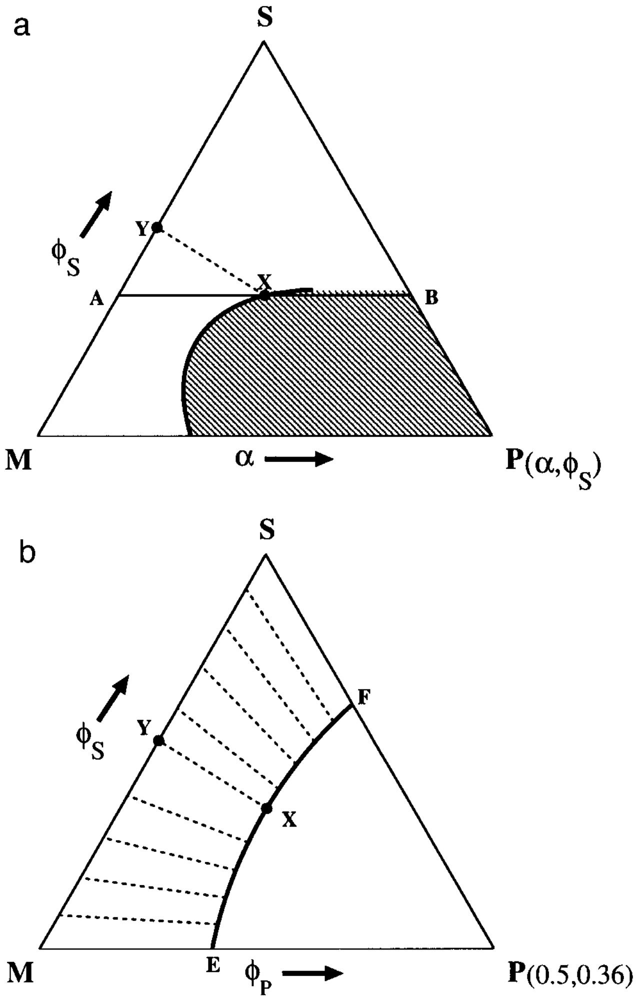

**Figure 2.** (a) Conversion−phase diagram for the case $\chi_{MP} = \chi_{MS} = \chi_{PS} = 0.5$. The polymerization line AB at $\phi_S = 0.36$ is drawn; it crosses the phase separation curve at point *X* ($\alpha = 0.5$, $\phi_S = 0.36$); at that point a new phase appears of composition *Y*. Notations are as in Figure 1a. (b) Ternary phase diagram of a polymer formed at point *X* in Figure 2a, in equilibrium with solvent and monomer. Notations are as in Figure 1b.

of 10 strongly changes the conversion−phase diagram. On further reduction, the upper phase transition line moves to still higher values of $\phi_S$ and no phase transition is observed if we disregard elasticity. However, if one disregards elasticity but changes the $\chi$ parameters, one can produce a phase separation line similar to the one in Figure 3, as illustrated in Figure 4. Note that in the system of Figure 4, the polymer structure is independent of conversion (no network, $r_P = \infty$), so that the conversion−phase diagram is identical to the phase diagram. We conclude that elasticity is important but that it may still be difficult to distinguish the effects of elasticity and of $\chi$ parameters in PIPS experiments.

One may wonder what happens after phase separation. After phase separation, the volume of the network phase is smaller than the total volume of the system, so that the polymer volume fraction of the network phase is not equal to the overall polymer volume concentration. This leads to an extra unknown; the extra equation is given by demanding that the chemical potential of the polymer in the network phase is zero. The network term is complicated by the fact that the shrinkage of the polymer phase after polymerization leads to a network that has portions created at different polymer volume fractions $\Phi_P$. This has been discussed by Dušek.[13] Another complication is that polymerization will continue in both phases. It has been observed[39] that this may lead to secondary phase separation. The treatment of this situation is beyond the scope of the present paper.

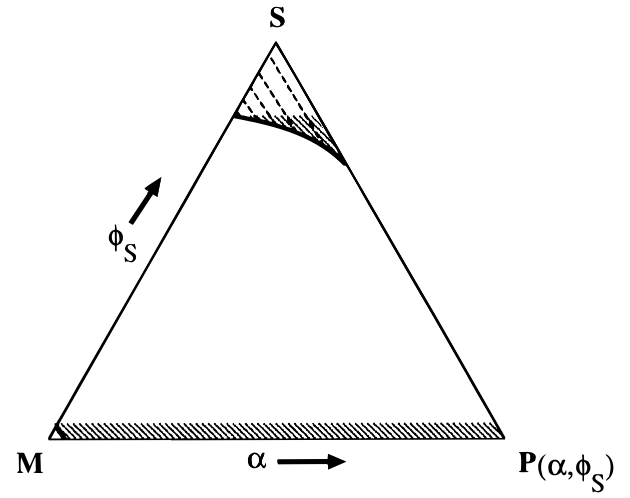

**Figure 3.** Conversion−phase diagram for the case $\chi_{MP} = \chi_{MS} = \chi_{PS} = 0.5$ where the elasticity is reduced by an efficiency factor of 0.1. For several points on the phase separation curve, the compositions of the two phases are indicated by dashed connecting lines. Phase separation occurs in two different regions of the diagram (shaded in the figure).

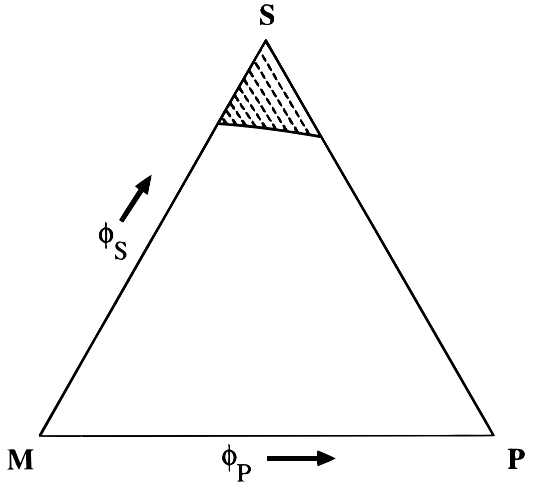

**Figure 4.** Phase diagram for the case $\chi_{MP} = 0.5$, $\chi_{MS} = \chi_{PS} = 0.6$ if the elasticity is disregarded and $r_P$ is taken infinite. For several points on the phase separation curve, the compositions of the two phases are indicated by dashed connecting lines.

## 7. Conclusion

In the literature on the formation of PDLCs by polymer-induced phase separation, network elasticity has so far not been taken into account. In this paper we stress the importance of elasticity: it may induce the phase separation.

The phase behavior during polymerization cannot be described in a single, true phase diagram, since the structure and size of the polymer component change by the reaction. Therefore, we use a conversion−phase diagram to visualize the elasticity-induced phase transition. In the following paper we shall use these diagrams to show that the model of elasticity-induced phase separation provides a qualitative explanation of our experiments.

## Appendix

This Appendix contains some generalizations of the model of section 2.

**Unequal Sizes of Monomer, Solvent, and Polymer.**[24] The Flory–Huggins expression for the free energy of a mixture of molecules of sizes $r_M$, $r_S$, and $r_P$ per unit size is a trivial extension of eq 2,

$$\frac{\Delta G^{\rm mix}}{Nk_BT} = \frac{\phi_M}{r_M}\log\phi_M + \frac{\phi_S}{r_S}\log\phi_S + \frac{\phi_P}{r_P}\log\phi_P + \sum_{ij}\chi_{ij}\phi_i\phi_j \tag{17}$$

It is easiest to consider each molecule of type $i$ as being placed on $r_i$ lattice sites of unit size. A repeat unit in a polymer molecule is of monomeric size and occupies $r_M$ sites; a polymer molecule consists of $r_P/r_M$ repeat units. If $N_i$ is the number of molecules of type $i$, then $N = r_MN_M + r_SN_S + r_PN_P$ is the total number of sites in the system. The mixing chemical potential related to adding one monomer molecule to the system is given by the derivative of $\Delta G^{\rm mix}$ to $N_M$. The result is a minor generalization of eq 3,

$$\Delta\mu_M^{\rm mix}/(k_BT) = \log\phi_M + \left(1 - \frac{r_M}{r_S}\right)\phi_S + \left(1 - \frac{r_M}{r_P}\right)\phi_P + r_M[\chi_M(1-\phi_M)^2 + \chi_P{\phi_P}^2 + \chi_S{\phi_S}^2] \tag{18}$$

and similarly for the solvent chemical potential. Now $r_P$ is the number of units of unit size in a polymer molecule; the number of repeat units of monomer in the polymer is $r_P/r_M$.

The elastic chemical potential for a monomer of size $r_M$ is obtained by multiplying the right-hand side of eq 7 by $r_M$, while the elastic chemical potential of the solvent is obtained by multiplying by $r_S$.

**Qualitative Effect of Modern Models of Lattice Elasticity.** Over the years many models of rubber elasticity have been proposed. Petrović *et al.*[18,25] suggested one estimate the qualitative effect of these models by imposing a linear dependence of $A$ and $B$ on the polymer volume fraction with limiting values corresponding to the model of Flory and Erman,[15]

$$A = 1 - 2(1 - \phi_P)/f \qquad B = 2\phi_P/f \tag{19}$$

Differentiation with respect to $N_M$ or $N_S$ leads to[18]

$$\Delta\mu_M^{\rm el}/(k_BT) = \Delta\mu_S^{\rm el}/(k_BT) = {m_c}^{-1}\left[{\Phi_P}^{2/3}A{\phi_P}^{1/3} - \frac{3}{f}({\Phi_P}^{2/3}{\phi_P}^{4/3} - {\phi_P}^2) - B(1 + \ln\phi_P)\right] \tag{20}$$

If we consider the microgel particles as our effective cross-links of very high functionality, this model becomes identical to model B of section 4. For finite values of $f$, we checked that the results do not differ qualitatively from the results of the affine elasticity model in the bulk of this paper.

## References and Notes

(1) Doane, J. W.; Golemme, A.; West, J. L.; Whitehead, J. B.; and Wu, B.-G. *Mol. Cryst. Liq. Cryst.* **1988**, *165*, 511.

(2) Kelly, J. R.; Palffy-Muhoray, P. *Mol. Cryst. Liq. Cryst.* **1994**, *243*, 11.

(3) Drzaic, P. S. *Liquid Crystal Dispersions*; World Scientific: Singapore, 1995.

(4) Hirai, Y.; Niiyama, S.; Kumai, H.; Gunjima, T. *SPIE* **1990**, *1257*; *Rep. Res. Lab., Asahi Glass Co., Ltd.* **1990**, *40*, 285.

(5) Smith, G. W. *Int. J. Mod. Phys. B* **1993**, *7*, 4187.

(6) Kim, J. Y.; Cho, C. H.; Palffy-Muhoray, P.; Mustafa, M.; Kyu, T. *Phys. Rev. Lett.* **1993**, *71*, 2232. Shen, C.; Kyu, T. *J. Chem. Phys.* **1995**, *102*, 556.

(7) Serbutoviez, C.; Kloosterboer, J. G.; Boots, H. M. J.; Touwslager, F. J. *Macromolecules* **1996**, *29*, 7690 (following article in this issue).

(8) James, H. M.; Guth, E. *J. Chem. Phys.* **1943**, *11*, 455, 472.

(9) Flory, P. J.; Rehner, J. *J. Chem. Phys.* **1943**, *11*, 521.

(10) Hermans, J. J. *Trans. Faraday Soc.* **1947**, *43*, 591.

(11) Flory, P. J.; Wall, F. T. *J. Chem. Phys.* **1950**, *18*, 108.

(12) Dušek, K.; Prins, W. *Adv. Polymer Sci.* **1969**, *6*, 1.

(13) Dušek, K. *J. Polym. Sci. C* **1967**, *16*, 1289.

(14) Staverman, A. J. In *Handbuch der Physik XIII*; Flügge, S., Ed.; Springer: Berlin, 1962.

(15) Flory, P. J.; Erman, B. *Macromolecules* **1982**, *15*, 800.

(16) Everaers, R.; Kremer, K. *Macromolecules* **1995**, *28*, 7291 and references therein.

(17) Goossens, J. G. P.; Rastogi, S.; Meijer, H. E. H.; Lemstra, P. J. *Polymer*, submitted for publication.

(18) Moerkerke, R.; Koningsveld, R.; Berghmans, H.; Dušek, K.; Šolc, K. *Macromolecules* **1995**, *28*, 1103.

(19) Recent references citing earlier literature include: Shen, C.; Kyu, T. *J. Chem. Phys.* **1995**, *102*, 556. Dorgan, J. R. *Fluid Phase Equilib.* **1995**, *109*, 157. Lansac, Y.; Fried, F.; Maïssa, P. *Liq. Cryst.* **1995**, *18*, 829.

(20) Gee, G.; Herbert, J. B. M.; Roberts, R. C. *Polymer* **1965**, *6*, 541. Brotzman, R. W.; Eichinger, B. E. *Macromolecules* **1981**, *14*, 1445. Neuburger, N. A.; Eichinger, B. E. *Macromolecules* **1988**, *21*, 3060. Zhao, Y.; Eichinger, B. E. *Macromolecules* **1992**, *25*, 6988.

(21) Pekarski, P.; Rabin, Y.; Gottlieb, M. *J. Phys. II Fr.* **1994**, *4*, 1677.

(22) Flory, P. J. *J. Chem. Phys.* **1941**, *9*, 660. Huggins, M. L. *J. Chem. Phys.* **1941**, *9*, 440. Staverman, A. J.; van Santen, J. H. *Recl. Trav. Chim. Pays-Bas* **1941**, *60*, 76.

(23) The factor $A$ may, in principle, depend on the quality of the solvent–monomer mixture as a solvent for the polymer.[13] This effect is neglected.

(24) Tompa, H. *Polymer Solutions*; Butterworth: London, 1956.

(25) Petrovič, Z. S.; MacKnight, W. J.; Koningsveld, R.; Dušek, K. *Macromolecules* **1987**, *20*, 1088.

(26) Dušek, K. *J. Polym. Sci. C* **1972**, *39*, 83. Dušek, K. *J. Polym. Sci., Polym. Phys. Ed.* **1974**, *12*, 1089.

(27) Around the critical point, one can always find a small region where the value of $r_P$ matters even if $r_P$ is very large.[24]

(28) Dušek, K. In *Developments in Polymerization – 3*; Haward, R. N., Ed.; Applied Science Publishers: London, 1984; Chapter 4.

(29) Mishra, V.; Du Prez, F. E.; Gosen, E.; Goethals, E. J.; Sperling, L. H. *J. Appl. Polym. Sci.* **1995**, *58*, 331.

(30) Kast, H.; Funke, W. *Makromol. Chem.* **1979**, *180*, 1335.

(31) Weiss, N.; van Vliet, T.; Silverberg, A. *J. Polym. Sci., Polym. Phys. Ed.* **1979**, *17*, 2229.

(32) Whitney, R. S.; Burchard, W. *Makromol. Chem.* **1980**, *181*, 869.

(33) Dušek, K.; Galina, H.; Mikeš, J. *Polym. Bull.* **1980**, *3*, 19.

(34) Kloosterboer, J. G.; van de Hei, G. M. M.; Boots, H. M. J. *Polym. Commun.* **1984**, *25*, 354.

(35) Micali, N.; Vasi, C.; Mallamace, F.; Bansil, R.; Pjevic, S.; Sciortino, F. *Phys. Rev. E* **1993**, *48*, 4501.

(36) Matsumoto, A. *Adv. Polym. Sci.* **1995**, *123*, 41.

(37) Dušek, K. In *Polymer Networks, Structure and Mechanical Properties*; Chompff, A. J., Newman, S., Eds.; Plenum Press: New York, 1971.

(38) Rehage, G. *Kolloid Z. Z. Polym.* **1964**, *194*, 16.

(39) Kloosterboer, J. G.; Serbutoviez, C.; Touwslager, F. J. *Liq. Cryst.*, in press.

MA960292H